6-1-1992

ADAPTIVE CONTROL OF KINEMATICALLY REDUNDANT ROBOTS

Shengwu Luo,
Purdue University School of Electrical Engineering

Shaheen Ahmad
Purdue University School of Electrical Engineering

Mohamed Zribi
Purdue University School of Electrical Engineering

ADAPTIVE CONTROL OF KINEMATICALLY CONTROLLED REDUNDANT ROBOTS

SHENGWU LUO
SHAHEEN AHMAD
MOHAMED ZRIBI

TR-EE 92-22
JUNE 1992

SCHOOL OF ELECTRICAL ENGINEERING
PURDUE UNIVERSITY
WEST LAFAYETTE, INDIANA 47907-1285

ADAPTIVE CONTROL OF KINEMATICALLY REDUNDANT ROBOTS

Shengwu Luo, Shaheen Ahmad and Mohamed Zribi

Real-Time Robot Control Laboratory
School of Electrical Engineering, Purdue University
West Lafayette, IN 47907-1285, USA

Abstract

A redundant robot has more degrees of freedom than what is needed to uniquely position the robot end-effector. In a usual robotic task, only the end-effector position trajectory is specified. The joint position trajectory is unknown, and it must be selected from a self-motion manifold for a specified end-effector. In many situations the robot dynamic parameters such as link mass, inertia and joint viscous friction are unknown. The lack of knowledge of the joint trajectory and the dynamic parameters make it difficult to control redundant robots.

In this paper, we show through careful problem formulation that the adaptive control of redundant robots can be addressed as a reference velocity tracking problem in the joint space. A control law which ensures the bounded estimation of the unknown dynamic parameters of the robot, and the convergence to zero of the velocity tracking error is derived. In order to ensure that the joint motion on the self-motion manifold remains bounded, a homeomorphic transformation is found. This transformation decomposes the velocity tracking error dynamics into a cascade system consisting of the dynamics in the end-effector error coordinates and the dynamics on the self-motion manifold. The dynamics on the self-motion manifold is directly shown to be related to the concept of ***zero-dynamics.*** It is shown that if the reference joint trajectory is selected to optimize a certain type of objective functions, then stable dynamics on the self-motion manifold results. This ensures the overall stability of the adaptive system. Detailed simulations are given to verify the theoretical developments. The proposed adaptive scheme does not require measurements of the joint accelerations or the inversion of the inertia matrix of the robot.

1. Introduction

A redundant robot is one which has more joints than what is required to poeition the end-effector. The extra joints can be used to configure the manipulator posture, to avoid obstacles in the workspace or to avoid joint singularities. Initial interest in the control of redundant robots started with the work of Whitney [28] who devised the kinematical resolved motion rate control. Liegeois et al. [15] formulated a kinematic control which optimized an objective function to avoid obstacles and joint eingularities. Their control scheme added a term (the so called null space term), which was used to produce the joint motion without affecting the end-effector motion. Since then several researchers have addressed the problem of kinematic motion coordination of redundant robots; see Nenchev [18] for a review of those developments. The tutorial review by Siciliano [24] and the tutorial workshop report on the theory and application of redundant robots covered some more recent develbpments. Recently, a handful of researchers took into account the dynamic model of the manipulator when they addressed the control problem of redundant robots. One of the first papers to rigorously address the redundant robot system stability while taking into account the dynamic model, was the paper by Hsu et al. [10]. They showed that it was necessary to ensure that the redundant joints contributing to the velocity in the null space exhibit stable behavior. To achieve this, they proposed a control law that included a null space term. In an effort to minimize the joint torque for redundant robots, Nakamura and Hanafusa [17] proposed an optimal control law which minimized the integral of the joint torque. De Luca [6] used the notion of zero dynamics to investigate the control and stability of redundant robot motions. Baillieul et al. [3] also addressed the problem of controlling redundant robots.

Recently a tremendous research effort has been directed toward the area of adaptive control of non-redundant rigid joint robots. These efforts are summarized in the survey papers written by Ortega and Spong [20] and Abdallah et al. [1]. Despite this progress it remained difficult to extend the adaptive control techniques of non-redundant rigid joint robots to the redundant robots case. This is the case because no explicit knowledge of the desired joint positions is available, usually only the end-effector path is given. As the redundant robot can assume an infinite set of joint positions for a given end-effector position, joint positions must be selected to ensure that the manipulator does not become singular. Further it is necessary to ensure stable motion of the joints while the end-effector tracks a desired trajectory.

In the area of redundant robot adaptive control, Seraji [23] presented an approach based on the model reference adaptive control theory. He resolved the redundancy problem by the so-called "configuration control scheme". The end-effector coordinates were augmented with functionally independent kinematic functions so that the resulting task-space configuration vector was of the same dimension as the joint vector, (therefore the joint solutions were unique). Hence the corresponding augmented Jacobian relating the velocities of the end-effector and the joints was a square matrix. Seraji's direct adaptive control scheme required the invertibility of the augmented Jacobian. Niemeyer and Slotine [19] applied sliding mode adaptive control to redundant manipulatore. They used the passivity principle to prove the stability of the adaptive system. In their echeme, through knowledge of the end-effector Cartesian reference velocity $\dot{x}_r$ and the performance index H, a reference joint velocity $\dot{q}_r$ and acceleration $\ddot{q}_r$ were obtained. The reference joint velocity and the reference joint acceleration were used in the control law. Niemeyer and Slotine also performed some experiments to demonstrate their control law. In depth stability analysis of the null space motion was not carried out by Seraji or Niemeyer and Slotine in their respective papers. Colbaugh et al. [5] proposed an adaptive inverse kinematics algorithm that did not require the knowledge of the kinematics of the robots. However their algorithm required persistent excitation conditions; also their algorithm did not consider the dynamics of the robot.

Middelton and Goodwin [16] proposed an adaptive computed torque control scheme for non-redundant robots. Their control law did not require the measurement of the joint accelerations. The convergence of the adaptive system was well proven. We made an attempt to extend Middelton and Goodwin's least square estimation based adaptive computed torque control law to redundant rigid manipulators. This attempt was not successful since the L^2 convergence of the prediction error in this scheme was not sufficient to ensure the asymptotic convergence of the redundancy resolution algorithms. Several researchers such as Bayard and Wen [4], Illchmann and Owens [11], Sadegh and Horowitz [22] and Song et al. [25] proposed several exponentially stable adaptive algorithms for the control of rigid link and rigid joint non-redundant manipulators. These algorithms did not require persistent excitation conditions for exponential convergence of the joint tracking error, and hence it is possible that the basic ideas behind these control schemes may be developed further for redundancy resolution.

This paper is organized in seven sections. In section 2, the redundancy resolution is discussed, and a model for the redundancy resolution is developed. The redundancy resolution problem is formulated as a differential equation involving the joint velocity tracking a computed reference signal. In section 3, an adaptive control scheme that leads to the convergence of the joint velocity tracking error is derived. This velocity tracking scheme is based on the redundancy resolution scheme formulated in section 2. In section 4, we investigate the boundedness of the joint motions and the boundedness of the control torques. The boundedness of the velocity tracking error leads to a differential equation perturbed by decaying term. We show that the boundedness of the decayed perturbation system is guaranteed by the boundedness of the solution of the unperturbed system. In section 5, The overall stability of the adaptive redundancy resolution algorithm is discussed. We find that the overall stability can be investigated in two parts as the unperturbed system can be transformed into a cascade system. One component of the cascade system corresponds to the dynamics on the self-motion manifold, the other component corresponds to the dynamics in the end-effector coordinates. Connections between the well established concept of zero dynamics and the joint dynamics on the self-motion manifold, are also shown in section 5. The overall stability of the adaptive system is proved for a class of objective functions used for redundancy resolution. In section 6, the performance of the adaptive system is evaluated through **simulations** and numerical verification of theoretical results. Finally, summary and conclusions are given in section 7.

2. Asymptotic Resolution of the Redundancy

2.1 Some Prerequisites

Consider a kinematically redundant manipulator with the end-effector positioned in the workspace at point $x \in X$, and the joints positioned in the joint space at $q \in Q$ The differentiable kinematic mapping relating x and q is $K: Q \rightarrow X$ such that,

$$x = K(q) \tag{1}$$

with the workspace $X \subset IR^m$ and the joint space $Q \subset IR^n$ and $m < n$. Further the degree of redundancy is $r = n-m$. Therefore for an end-effector point $x = x_0$ in the workspace, there exists a set of joint positions, Q_N, which lie on the self-motion manifolds in the joint space such that $Q_N = \{q \in Q \mid x = x_0 = K(q)\}$. In order to determine a unique solution of the joint vector additional requirements on the joint vector must be found. In order to do this, we will state several properties of the kinematic mapping given by **(1).** We will denote the Jacobian of the kinematic map by† $J(q)$, $J = \frac{\partial K}{\partial q} \in IR^{m \times n}$. Further we note the relationship between the end-effector and joint velocities, as,

$$\dot{x} = J\dot{q}. \tag{2}$$

Thus, if I_n is the n by n identity matrix then the projection operator onto the null space of J is denoted by $P_J(q) = I_n - J^+ J \in IR^{n \times n}$, and the right inverse of J (assuming $\text{rank}(J) = m$) will be denoted as $J^+ = J^T(JJ^T)^{-1}$. We will let all the columns of the matrix $N_J(q) \in IR^{n \times r}$ be the normalized bases of $ker(J)$, ($ker(J)$ is the null space of J. Hence we have,

$$JP_J = 0, \qquad \text{and} \qquad ker(J) = span(N_J) \tag{3}$$

The bases vectors of the matrix N_J represent the local tangents of the self-motion manifold Q_N. The matrix N_J has the following properties,

$$JN_J = 0 \in IR^{m \times r}\ ,\quad N_J^T J^T = 0 \in IR^{r \times m}\ ,\quad N_J^T J^+ = 0 \in IR^{r \times m}\ ,$$

$$N_J^T P_J = N_J^T\ ,\quad N_J^T N_J = I_r \in IR^{r \times r}\ ,\quad N_J N_J^T = P_J \in IR^{n \times n}\ ;$$

for any vector $\dot{q} \in IR^n$ **if** $N_J^T(q)\dot{q} = 0 \in IR^r$ **then** $P_J(q)\dot{q} = 0 \in IR^n$. **(4)**

Notice also that the matrix $\begin{bmatrix} J \\ N_J^T \end{bmatrix}$ is a square matrix of full rank, thus we have,

$$\begin{bmatrix} J \\ N_J^T \end{bmatrix}^{-1} = [J^+ \;\; N_J]\ . \tag{5}$$

From the above properties we can conclude that the pairs (J, N_J^T) and (J^+, N_J) are orthogonal complement operator pairs.

† Note that we will drop functional dependencies whenever it is possible.

2.2 Statement of the Redundancy Resolution Problem

A joint position q can be found from the specification of the end-effector position x and the optimization of an objective function $H(q)$. This is known as the redundancy resolution, and it results in a constrained optimization of the objective function H. The problem can be formulated as follows, given a desired position x_d, find the joint position q such that,

$$\min_{q} \quad H(q) \qquad \text{subject to} \quad x_d = K(q) \,. \tag{6}$$

We can conclude from the **Lagrange** multiplier method that the necessary condition for the optimization of problem (6) satisfies the following set of "constrained" differential equations:

$$P_J(q)\nabla H(q){=}0 \qquad \textit{and} \qquad x_d{=}K(q) \,. \tag{7}$$

To develop the control problem, we will define the end-effector path tracking error, e, as

$$e{:=}K(q){-}x_d = x{-}x_d \,, \tag{8}$$

then we desire the "asymptotic resolution of the redundancy problem" such that, $\dot{e}\rightarrow 0$, $e\rightarrow 0$, and $P_J(q)\nabla H(q)\rightarrow 0$ as $t \rightarrow \infty$. We want to optimize $H(q)$ by appropriate joint motion on the self-motion manifold, Q_N. At the optimal point, we do not desire further motion on the self-motion manifold. Therefore the projection of the joint velocity on the self-motion manifold must be zero, and $N_J^T\dot{q} \rightarrow 0$ as $t \rightarrow \infty$. Hence, it is sufficient (not necessary) to write the asymptotic redundancy resolution as $t\rightarrow\infty$,

$$\begin{aligned} &\dot{e}+\gamma e\rightarrow 0 \\ &N_J^T(\dot{q}-\lambda\nabla H)\rightarrow 0 \,, \qquad \text{with} \qquad N_J^T\dot{q}\rightarrow 0 \,. \end{aligned} \tag{9}$$

Where, $\gamma > 0$ and $\lambda\neq 0$ are some constants. The first equation above can be written as $J\dot{q}-\dot{x}_d+\gamma e\rightarrow 0$. After grouping terms and using the matrix inversion result in (5), we get, as $t\rightarrow\infty$,

$$\dot{q}-\begin{bmatrix} J^+ & N_J \end{bmatrix}\begin{bmatrix} \dot{x}_d-\gamma e \\ \lambda N_J^T\nabla H \end{bmatrix}\rightarrow 0 \qquad \text{with} \qquad q\rightarrow\{q\in Q \mid N_J^T\nabla H{=}0 \text{ and } K(q){=}x_d\} \tag{10}$$

Therefore the "asymptotic resolution of the redundancy problem" can be expressed by the conditions on the differential equations given by (10). These conditions result in the joint velocity vector approaching its desired value, meanwhile the joint position vector would be at the solution of a set of constraint equations. Notice that the redundancy resolution problem is characterized by the fact that ***the desired joint positions are unknown in advance.*** This fact prevents us from directly using the existing adaptive schemes that achieve joint position tracking.

Now by denoting $u \in IR^n$ as,

$$v{=}\begin{bmatrix} J^+ & N_J \end{bmatrix}\begin{bmatrix} \dot{x}_d-\gamma e \\ \lambda N_J^T\nabla H \end{bmatrix} , \tag{11}$$

the asymptotic redundancy resolution of the problem can be solved by a scheme that ensures the velocity tracking error $\dot{q}-v \rightarrow 0$, as $t \rightarrow \infty$. In the next section we will develop such an adaptive scheme.

3. Parameter Update Law and the Control Law

3.1 Dynamic Model and Properties

The dynamics of a rigid robot with n joints can be represented explicitly in terms of the structural parameters by the following Euler-Lagrange equation :

$$\tau = D(q;\theta)\ddot{q}+C(q,\dot{q};\theta)\dot{q}+g(q;\theta)\ , \tag{12}$$

where, $\theta \in IR^{a}$ is the vector of structural parameters of the manipulator and a is the number of unknown parameters. The inertia matrix is $D \in IR^{nXn}$. Further, $C \in IR^{mXn}$ is the Coriolis and centrifugal matrix, and $g \in IR^{n}$ is the gravitational force term. The dynamics of the manipulator has the following properties,

(P1) Positive definiteness of the inertia matrix,

$$D(q;\theta)=D^{T}(q;\theta) > 0 \quad \text{with} \quad \theta \in IR^{a} \quad \text{and} \quad q \in IR^{n} \tag{13}$$

(P2) Skew-symmetry of the matrix $\dot{D}-2C$ [26],

$$\rho^{T}\left(\dot{D}(q;\theta)-2C(q,\dot{q};\theta)\right)\rho = 0, \quad \text{for any } \rho \in IR^{n}\ . \tag{14}$$

(P3) Linear parameterization of the dynamical equations.

The Euler-Lagrange equation (12) is linear with respect to the structural parameters θ ([1, 20]), hence,

$$D(q;\theta)\ddot{q} + C(q,\dot{q};\theta)\dot{q} + g(q;\theta) = Y(q,\dot{q},\ddot{q})\theta. \tag{15}$$

Further, we can show that [26],

$$D(q;\theta)a+C(q,\dot{q};\theta)v+g(q;\theta)=Y(q,\dot{q};v,a)\theta\ . \tag{16}$$

Here the vectors v and a $\in IR^{n}$. The regressor matrix $Y(.) \in IR^{nX*}$ is known. The matrix Y and the vectors a and v are independent of the structural parameters θ. Notice that it is not necessary to satisfy $a = \dot{v}$.

A similar relation to (16) holds when the estimates of the parameters $\hat{\theta}$ are used to replace the exact parameters θ, i.e.,

$$\hat{D}a+\hat{C}v+\hat{g}=Y(q,\dot{q};v,a)\hat{\theta} \tag{17}$$

where for brevity we have denoted $\hat{D}:=D(q;\hat{\theta})$, $\hat{C}:=C(q,\dot{q};\hat{\theta})$ and $\hat{g}:=g(q;\hat{\theta})$.

3.2 Control Law Derivations

Now consider a control torque of the form,

$$\tau = \hat{D}a+\hat{C}v+\hat{g}-K_{r}(\dot{q}-v)\ , \tag{18}$$

where the matrix $K_{r}=K_{r}^{T} > 0$. Using (12), (16), (17) and (18), this control torque leads to the following composite (error) system:

$$D(\ddot{q}-a)+C(\dot{q}-v)+K_r(\dot{q}-v)=Y(q,\dot{q};v,a)(\hat{\theta}-\theta)=Y\tilde{\theta}, \tag{19}$$

where the parameter error is defined as $\tilde{\theta}:=\hat{\theta}-\theta$. The vectors a and v in equation (18) will be determined in a way to resolve the redundancy.

The convergence of the above control law can be improved (this will be seen later), if we use a scalar positive time increasing function w_t as follows,

$$\rho:=w_t(\dot{q}-v) \quad \text{and} \quad \dot{\rho}:=w_t(\ddot{q}-a)\ . \tag{20}$$

Then the composite system (19) can be written as,

$$D\dot{\rho}+C\rho+K_r\rho=Y(q,\dot{q};v,a)\tilde{\theta}w_t\ . \tag{21}$$

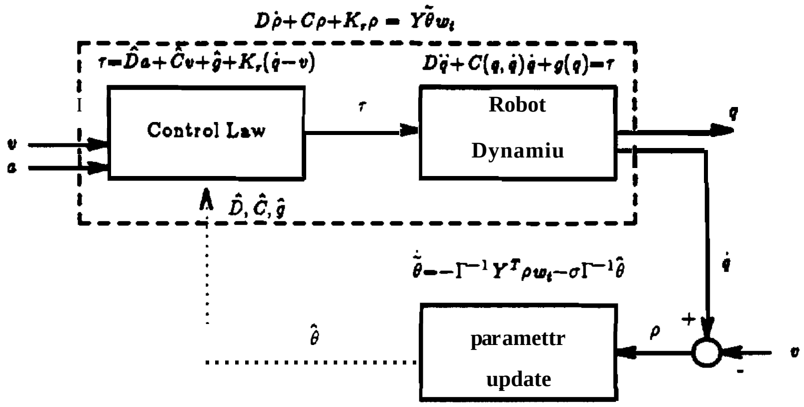

Fig. 1 The Structure of the Adaptive Control Scheme

The next theorem asserts that the stability of the above closed loop system is guaranteed when the following parameter update law is used:

$$\dot{\tilde{\theta}}=\dot{\hat{\theta}}=-\Gamma^{-1}Y^T\rho w_t-\sigma(t)\,\Gamma^{-1}\,\hat{\theta}\ , \tag{22}$$

where the constant gain matrix $\Gamma=\Gamma^T>0$. The "a–modification" scheme [12] is used to prevent the drift of the parameter estimates in an unbounded manner in the presence of unmodeled disturbances. The scalar function $\sigma(t)$ is chosen as,

$$\sigma(t)=0 \qquad if \quad ||\hat{\theta}||\le\bar{\theta}$$

$$\text{and,}\quad \sigma(t)=\sigma_0 \qquad \text{if} \quad ||\hat{\theta}||>\bar{\theta} \tag{23}$$

where the constant $\bar{\theta}$ is an upper bound of the norm of the actual parameters, such that $\bar{\theta}>||\theta||$, and a, is a positive constant.

<u>Theorem 1</u> (The stability of the closed loop adaptive system.)

The control torque (18) and the parameter update law (22) when applied to the dynamic system given by (12), achieve a bounded stable closed loop system such that $\rho\in L^2\cap L^\infty$ and 8 $\in L^\infty$ (see Fig. 1 for depiction of the control scheme). O

Proof : Consider the Lyapunov function candidate V defined by, $V:=\frac{1}{2}\rho^T D\rho+\frac{1}{2}\tilde{\theta}^T\Gamma\tilde{\theta}$, then by using properties (P1) - (P3) and equations (21) and (22), it is easy to show that, $\dot{V}=-\rho^T K_r\rho-\sigma(t)(\hat{\theta}-\theta)^T\hat{\theta} \leq -\rho^T K_r\rho \leq 0$. This is true because the term $-\sigma(t)(\hat{\theta}-\theta)^T\hat{\theta}$ is non-positive as,

$$-\sigma(t)(\hat{\theta}-\theta)^T\hat{\theta}\leq -\sigma(t)||\hat{\theta}||^2+\sigma(t)||\hat{\theta}||\ ||\theta|| \leq -\sigma(t)||\hat{\theta}||\ (\ ||\hat{\theta}||-\bar{\theta}\ )\leq 0\ .$$

As the Lyapunov function V is globally positive definite and radially unbounded for $(\rho,\tilde{\theta})$, and the matrices D, Γ and K_r are positive definite, we have $\rho \in L^2\cap L^\infty$ and $\tilde{\theta} \in L^\infty$ for the system given by (12), (18) and (22). ●

We now define the velocity tracking error δ_v as,

$$\delta_v(q,t):=\dot{q}-v\ . \tag{24}$$

The convergence of $\dot{q}-v=w_t^{-1}\rho$ to zero is guaranteed by the boundedness of ρ, and it can be improved by specifying the scalar time dependent function w_t in (20).

Corollary 1 (The type of stability is determined by w_t.)

If w_t is a scalar time increasing function, then $\delta_v=(\dot{q}-v)\rightarrow 0$ at the rate of w_t^{-1}. If w_t^{-1} is an integrable function, then $(\dot{q}-v)$ belongs to L^1 and $(\dot{q}-v)\rightarrow 0$, as $t\rightarrow\infty$. The integrable functions from which w_t can be chosen, include the exponential function and functions of the form,

$$w_t(t)=(t+1)^{1+\alpha} \quad \text{with} \quad \alpha > 0\ . \tag{25}$$

Furthermore if $w_t=\exp(bt)$, then $(\dot{q}-v)\rightarrow 0$ at the rate of $\exp(-bt)$.

Proof : The results immediately follows from the fact that $(\dot{q}-v)=\rho w_t^{-1}$. As $\rho(t)$ is bounded by $B_\rho:=\sup_t ||\rho(t)||$, we have,

$$||\delta_v||=||\dot{q}-v(q)||\leq B_\rho w_t^{-1}\ . \tag{26}$$

Notice that the boundary function $\beta(t):=B_\rho w_t^{-1}$ is independent of q. Also notice that if w_t is given by (25), then $w_t^{-1}\in L^1$, since $\int_0^\infty \frac{dt}{(t+1)^{1+\alpha}}=1/\alpha < \infty$, therefore $\delta_v \in L^1$. If we select an exponential weighting function then from (26), we can immediately see that $\delta_v\rightarrow 0$ at the rate of $\exp(-bt)$. ■

Remark 1 : The transformation (20) between the reference acceleration, a, and the reference velocity, v, is :

$$a=\dot{v}-(\dot{q}-v)\dot{w}_t w_t^{-1}\ . \tag{27}$$

Notice that v is independent of $\dot{q}$ (see equation (11)), and hence a is not a function of $\ddot{q}$. Therefore the adaptive scheme does not require the measurement of the joint acceleration $\ddot{q}$.

O

From equation (11), the reference velocity, v, for redundant robots is given by,

$$v=J^+\ (\dot{x}_d-\gamma e)+\lambda P_J\nabla H\ . \tag{28}$$

Thus the reference acceleration becomes,

$$a=J^{+}(\ddot{x}_d-\gamma\dot{e})+\frac{dJ^{+}}{dt}(\dot{x}_d-\gamma e)+\lambda P_J\frac{d}{dt}\nabla H+\lambda\dot{P}_J\nabla H-[\dot{q}-J^{+}(\dot{x}_d-\gamma e)-\lambda P_J\nabla H]\dot{w}_t w_t^{-1} \ . \qquad (29)$$

Remark 2 : We have shown that if the adaptive control law given by equation (18) and (22) is used, we have $\dot{q}\rightarrow v$ as $t\rightarrow\infty$. However we have to show that q *is* bounded, and then we can conclude that $\dot{q}$ and $v(q)$ are bounded, which then ensures the boundedness of τ.

4. Boundedneee of the Joint Motions and Control Torques

4.1 Stability of the Perturbed System

In this section we will show that the boundedness of q, $\dot{q}$, and τ, is dependent on the stability of a perturbed differential equation. From the results of theorem 1 and equations (24) and (26), the velocity tracking error can be expressed as a perturbed dynamical system with a decaying perturbation, thus,

$$\dot{q}=v(q)+\delta_v(q,t) \ . \qquad (30)$$

Recall from corollary 1 that $||\delta_v(q,t)||\leq\beta(t)\rightarrow 0$, thus the perturbation δ_v is bounded and tends to zero as $t\rightarrow\infty$.

We will prove the boundedness of q in the perturbed system described by equation (30) by ensuring the boundedness of q in the unperturbed system given by $\dot{q}=v(q)$. In the following, we will establish the relationship between the boundedness of the perturbed and unperturbed systems. The first important result needed to achieve this is the result of Markus and Opial (see [8], p. 282).

Lemma (Stability of the perturbed system.) [8]

Consider the perturbed differential equation with f : $IR^n \rightarrow IR^n$ and z_δ, $\delta(z_\delta,t)\in IR^n$, such that,

$$\dot{z}_\delta=f(z_\delta)+\delta(z_\delta,t) \qquad with \quad z_\delta(0)=z^0 \ . \qquad (31)$$

This dynamic system is called "asymptotically autonomous" if (1) $\delta(z_\delta,t)\rightarrow 0$ as $t\rightarrow\infty$ uniformly for z_δ in an arbitrary compact set Ω in IR^n, or (2) $\delta(z_\delta,t)\in L^1$ for all $z_\delta(t)$ which are bounded and continuous on Ω for $t\geq 0$. Then, the positive limit sets (i.e., the set with $t\in IR+$ and $t\rightarrow\infty$) of the solutions of (31) are invariant sets of the original stable differential equation,

$$\dot{z}=f(z) \qquad \text{with} \quad z(0)=z^0 \ , \qquad (32)$$

where $z\in IR^n$. O

Recall that the set S is said to be an invariant set under the vector field $\dot{z}=f(z)$ if for any $z^0\in S$, we have $z(t,t_0,z^0)\in S$ for all $t\in IR^+$. Therefore if we choose $w_t^{-1}\in L^1$ then the redundancy resolution, equation (30), modeled as a perturbed system is indeed asymptotically autonomous, since the perturbation term $\delta_v\in L^1$, as

$||\delta_v||_{L^1}=\int_{u=0}^{\infty}||\delta_v||du \leq B_\rho \int_{u=0}^{\infty} w_t^{-1}du$. In the next lemma we will show that $||z_\delta-z||$ is bounded for $t \to \infty$. Finally in lemma 3 we will show that $||z_\delta-z||$ has a finite bound for all t.

Lemma 2 (Asymptotic stability of the perturbed system).

Assume that the perturbed system (31) is an asymptotically autonomous system. Then the limit solution set of (31) is the limit solution set of (32). If the positive limit set of (32) is bounded, then $||z_\delta-z||$ is bounded as $t \to \infty$. O

Proof:

Let V be a continuous Lyapunov function defined on the set $G \subset IR^n$. We define E to be the set of all points in the closure [21] of G, (the closure of G will be denoted by $\bar{G}$), where $\dot{V}(z)=0$, that is, $E=\{z \mid \dot{V}(z)=0, z \in \bar{G}\}$. Let M_E be the largest invariant set in E. Then LaSalle's invariance theorem [14] asserts that every solution of (32) approaches M_E as $t \to \infty$. Thus the result of lemma 1 yields that the positive limit set of (31) is the positive limit set of (32), hence z_δ tends to some limit points of the unperturbed system in (32). Moreover, if the positive limit set of (32) is bounded, then $||z_\delta-z||$ is bounded as $t \to \infty$. ■

From lemma 2, we can deduce that if Δ_h is the diameter of a ball which contains the limit set of (32) (i.e., $||z_\delta(t)-z(t)||<\Delta_h$ as $t \to \infty$), then given any number $h > \Delta_h$, we can always find a time t_h, such that for $t > t_h$ we have $||z_\delta(t)-z(t)||<h$. The next lemma enables us to show that the trajectory of (31) for $t \in [0, t_h]$ is bounded.

Lemma (Boundedness of the perturbed system).

Consider the perturbed differential equation (31) and suppose that the mapping $j: IR^n+IR^n$ has a Lipschitz constant $C_L > 0$ for $||z||<\infty$, and suppose that the perturbation $\delta_v(z_\delta, t)$ along the trajectory has bounded L^1 norm, i.e., $||\delta_v||_{L^1} = \int_0^\infty ||\delta_v(z_\delta, u)||du \leq B_\delta$, where B_δ is a positive constant. Then the trajectory $z_\delta(t)$ is bounded up to a given time t_h if the original differential equation (32) is stable. *O*

Proof : It is sufficient to show that $||z_\delta-z||$ is bounded for all $t \in [0,\infty)$, since $z(t)$ is bounded by the assumption of the stability of (32). The solution curve of (31) can be written as $z_\delta(t)-z^0=\int_{u=0}^{t} f(z_\delta)du + \int_{u=0}^{t} \delta(z_\delta,u)du$. Similarly for the unperturbed system (32), we have $z(t) - z^0 = \int_{u=0}^{t} j(z)du$. Combining these two equations, we get $z_\delta(t)-z(t)=\int_{u=0}^{t} \delta(z_\delta,u)du + \int_{u=0}^{t} (f(z_\delta)-f(z))\, du$. Here the function f(.) is Lipschitz by assumption, hence, $||z_\delta-z|| \leq B_\delta + \int_{u=0}^{t} C_L||z_\delta-z||du$. As the vector norm of the solutions of (31) and (32) are continuous and non-negative functions, therefore from the Bellman Gronwall lemma ([9] p. 168) we have,

$$||z_\delta - z|| \leq B_\delta e^{C_L t_h} \; , \tag{33}$$

for $t=t_h$. As the stability of the unperturbed system (32) ensures the boundedness of a, then z_δ is bounded for $t \in [0, t_h]$ and therefore for any given $t_h \in [0, \infty)$. ■

4.2 Boundedness of the Joint Motions

Using lemma 2 and lemma 3 to solve the asymptotic redundancy resolution problem, we arrive at the following propositions.

Proposition 1 (The boundedness of q and $\hat{\theta}$)

If we assume that the function $v(q)$ in (11) is Lipschitz, then we can find a set R_{q0} (the set of the initial joint positions) such that the solutions of the adaptive control system (i.e., the parameter estimates and the joint positions) are bounded for any time. Therefore with the adaptive control law given by (18) and (22), the solution of (12) is bounded for any time t, if the solution of the unperturbed system

$$J\dot{q} = \dot{x}_d + \gamma e, \quad and \quad N_J^T \dot{q} = \lambda N_J^T \nabla H \tag{34}$$

is bounded in R_{q0}. O

Proof : The adaptive system given by (12), (18) and (22) is an asymptotically autonomous system, as we have shown in corollary 1 that the perturbation term is a uniformly bounded time decreasing function. The set $\{q \mid ||\dot{q} - v(q)|| \leq B_\rho\}$ can be taken as the compact set Ω in lemma 1. Thus lemma 2 and lemma 3 guarantee the boundedness of the adaptive system for all t if q the solution of (34) is bounded. ■

The boundedness of the unperturbed system will be studied in the next section. To obtain the boundedness of the control torque, we require the following assumptions.

Assumptions

(A1) The desired paths $x_d(t)$, $\dot{x}_d(t)$ and $\ddot{x}_d(t)$ are bounded for all time t.

(A2) The Jacobian $J(q)$ is a full rank continuously differentiable function matrix, that is, $J(q)$ is of class C^r, $r \geq 2$ (i.e., at least twice differentiable).

(A3) The objective function $H(q)$ given in (6) is a twice differentiable real valued function.

In assumption (A2) the full rank restriction of $J(q)$ requires that all possible joint motions $q(t)$, solution of (34), do not pass through any joint configuration resulting in the singularity of $J(q)$. If $J(q)$ is continuous and full rank in a compact subset $G_J \subset \mathbb{R}^n$, then $J^+ = J^T(JJ^T)^{-1}$, $P_J = I_n - J^+ J$ and N_J are continuous in G_J. The matrices J, J^+, P_J and N_J are (shift varying) linear operators. It is easy to show that any continuous linear operator is bounded [21], hence J, J^+, P_J and N_J are bounded in Gj, i.e., the induced norm of J, J^+, P_J and N_J are finite on G_J. Furthermore, if $\dot{J}(q)$ is continuous in Gj, then $\frac{dJ^+}{dl} = -J^+ \dot{J} J^+ + P_J \dot{J}^T (JJ^T)^{-1}$, $\dot{P}_J = -\dot{J}^+ J - J^+ \dot{J}$ are continuous on any path with continuous $\dot{q}$ in G_J.

Proposition 2 (The boundedness of $\dot{q}$).

Based on assumptions (Al), (A2) and **(A3),** the boundedness of the joint position q ensures the boundedness of the joint velocity $\dot{q}$. O

Proof : The reference velocity v given by (28) is a function of x_d, $\dot{x}_d$ and q. By assumption (Al), the boundedness of q yields the boundedness of $\dot{x}_d-\gamma e$. By assumptions (A2) and **(A3),** the boundedness of q yields the boundedness of $J^+(q)$, $P_J(q)$ and $\nabla H(q)$, hence $v(q)$ is bounded for all bounded q. Therefore the boundedness of $||\dot{q}-v(q)||$ in the adaptive system leads us to the boundedness of $\dot{q}$, provided that q is bounded. ■

Proposition 3 (The boundedness of the control torque τ).

Based on assumptions (Al) and **(A2),** if q and $\dot{q}$ are bounded then the adaptive control torque defined by (18) is bounded. O

Proof : Based on assumptions (Al), (A2) and **(A3),** and the boundedness of q and $\dot{q}$, the reference velocity, v, and the reference acceleration, a, given by (28) and (29) respectively are bounded. Therefore the control torque is bounded. ■

5. The Stability of the Unperturbed System

5.1 Computation of the Self Motion Manifold and Zero Dynamics

In the below, we will examine the boundedness of the unperturbed system by using a homeomorphic transformation of the coordinates. Recall that a homeomorphismt maps a continuous function to another continuous function, and a homeomorphism preserves the topological properties such as the openness, connectedness, and the convergence of a set [21]. We will find a homeomorphism which transforms the joint coordinates q into a decomposable coordinates ξ and ς. Therefore the unperturbed system $\dot{q}=v(q)$ will be transformed into a cascade dynamic system, $\dot{\varsigma}=v_\varsigma(\varsigma,\xi)$, and $\dot{\xi}=v_\xi(\xi)$. It will be shown that ξ is homeomorphic to the workspace coordinates x. The variable ς will be used to represent the dynamics on the self-motion manifold. The boundedness of q will be deduced from the boundedness of ξ and ς. To find the homeomorphism, we will adopt the method used to prove the sufficiency of the Frobenius' theorem [13]. We will construct a diffeomorphism which is based on the self-motion manifold. For any given x, all the joint positions q such that $x=K(q)$, lie on the leaf of the self-motion manifold. (The leaf of the self-motion manifold, a sub-manifold, will be denoted by $Q_N^{x_0}$), this sub-manifold $Q_N^{x_0}$ **is** a connected region. By assumption $N_J(q)$ is nonsingular, thus the distribution $\Delta=ker\ (J)=$ span (Nj) is nonsingular. The null space of a regular Jacobian matrix is always completely integrable, hence A is involutive. The distribution A has an annihilator $\Delta^\perp$ which is spanned by J, and J is the exact differentials of the kinematic map K. The integrability of A allows us to construct the integral manifold by piecewise integration of every column of N_J.

† **A homeomorphiem is a continuous mapping between two topological spaces and its inverse mapping is also continuous.**

Let Φ_t^f denote the flow of the vector field f, such that $q(t)=\Phi_t^f(q_0)$ is the solution of the ordinary differential equation $\dot{q}=f(q)$ with the initial condition $q(0)=q_0$. The transition mapping Φ_t^f which maps q_0 to $q(t)$ is a diffeomorphism, and has the property $\frac{\partial\Phi_t^f(q_0)}{\partial t}=f(q(t))$ [9, 13]. The flow of each vector field, represented by a column of $N_J=[N_{J_1},\ldots,N_{J_r}]$, is the solution of the following differential equations,

$$\dot{q}=N_{J_i}(q) \qquad \text{with} \qquad q(0)=q_0, \quad \text{for } i=1,\ldots,r\,; \tag{35}$$

and can be written as, $q(t=\varsigma_i)=\Phi_{\varsigma_i}^{N_{J_i}}(q_0)$. Thus we have $\frac{\partial\Phi_{\varsigma_i}^{N_{J_i}}(q_0)}{\partial\varsigma_i}=N_{J_i}(q)$.

Lemma 4 (The parameterized equation of the self-motion manifold).
Given a kinematic mapping $x=K(q)$. The composite mapping Q_ς:IR^r+ Q_N :

$$(\varsigma_1,\cdots,\varsigma_r)\rightarrow q(t)=\Phi_{\varsigma_r}^{N_{J_r}}\circ\cdots\circ\Phi_{\varsigma_1}^{N_{J_1}}(q_0) \qquad \text{with} \quad t=\varsigma_1+\cdots+\varsigma_r\,. \tag{36}$$

is a locally parametrized equation of the manifold $Q_N^{q_0}=\{q\in C(q_0)\mid x_0=K(q)=K(q_0)\}$, which passes through q_0. Here $C(q_0)$ is used to denote the connected regions of the self-motion manifold and $C(q_0)$ passes through the initial joint configuration q_0. O

Proof : We shall show that for $t=\varsigma_1+\cdots+\varsigma_r$, $K(q(t))=K(q_0)$. Since $x=K(q)$, it suffices to show that x is unchanged whenever ς varies locally, i.e., $\frac{\partial x}{\partial\varsigma_i}=0$ for $i=1,\cdots,r$.

First, consider the rightmost integral $\Phi_{\varsigma_1}^{N_{J_1}}$ in (36). Let $q_{\varsigma_1}=\Phi_{\varsigma_1}^{N_{J_1}}(q_0)$, then,

$$\frac{\partial x}{\partial\varsigma_1}=\frac{\partial K}{\partial\varsigma_1}\Big|_{q_{\varsigma_1}}=\frac{\partial K}{\partial q}\Big|_{q_{\varsigma_1}}\bullet\frac{\partial q_{\varsigma_1}}{\partial\varsigma_1}=\frac{\partial K}{\partial q}\Big|_{q_{\varsigma_1}}\bullet\frac{\partial\Phi_{\varsigma_1}^{N_{J_1}}(q_0)}{\partial\varsigma_1}=J(q_{\varsigma_1})\,N_{J_{\varsigma_1}}(q_{\varsigma_1})=0\,.$$

Hence $q_{\varsigma_1}\in Q_N^{q_0}$ when $q_0\in Q_N^{q_0}$. Similarly, we have $\frac{\partial x}{\partial\varsigma_i}=0$ for $i=2,\cdots,r$. Then for the ith transition we have $q(t=\varsigma_1+\cdots+\varsigma_i)=\Phi_{\varsigma_i}^{N_{J_i}}(q(t=\varsigma_1+\cdots+\varsigma_{i-1}))$ and hence $q(t=\varsigma_1+\cdots+\varsigma_i)\in Q_N^{q_0}$. Moreover these q's are connected since $\Phi_{\varsigma_i}^{N_{J_i}}$ $(i=1,\cdots,r)$ are continuous mapping with respect to ς_i. Therefore (36) maps ς to $q(t)\in Q_N^{q_0}$. Furthermore, this mapping is a diffeomorphism because it is a composition of the diffeomorphisms $\Phi_{\varsigma_i}^{N_{J_i}}$. Hence this mapping satisfies to be a parameterization of the manifold. ■

Lemma 5 (Decomposition of the coordinates).
Given a kinematic mapping $x=K(q)$, let U be the image of the joint space Q. At any point $q\in Q\subset$ IR^n, there exists a diffeomorphism $F^{-1}:Q\rightarrow U\subset$ IR^n which decomposes q into $\varsigma\in IR^r$ and $\xi\in IR^m$, such that $\begin{bmatrix}\varsigma\\ \xi\end{bmatrix}=F^{-1}(q)$. The mapping $\varsigma(q)$ maps a point q on the self-motion manifold Q_N into ς. O

Proof : We will construct the desired diffeomorphism on the given leaf of the self-motion manifold. Recall that Nj is the orthogonal complement of the matrix J^+. Assuming that the matrix J is of full rank and has the right inverse J^+, $J^+=J^T(JJ^T)^{-1}$, then the range space of J^+ and the range space of J^T are equal. As the domain space of any matrix is the direct-sum of its row space and its null space, then the domain of J is IR^n, thus we have, $rank([N_J\,,\,J^+]) = n$. Consider the composite mapping F:U $\rightarrow$ Q such that,

$$(\varsigma_1, \cdots, \varsigma_r, \xi_1, \cdots, \xi_m) \rightarrow q(t) = \Phi^{J_m^+}_{\xi_m} \circ \cdots \circ \Phi^{J_1^+}_{\xi_1} \circ \Phi^{N_{J_r}}_{\varsigma_r} \circ \cdots \circ \Phi^{N_{J_1}}_{\varsigma_1}(q_0). \tag{37}$$

The mapping F is a diffeomorphism because the composition of diffeomorphisms is a diffeomorphism. Hence F^{-1}, the inverse of F, exists and is a smooth mapping. Thus,

$$\begin{bmatrix} \varsigma \\ \xi \end{bmatrix} = F^{-1}(q) \tag{38}$$

where $\varsigma=[\varsigma_1, \cdots, \varsigma_r]^T$ and $\xi=[\xi_1, \cdots, \xi_m]^T$ are real functions which are defined on U. ■

We have, $(\varsigma,\xi)=F^{-1} \circ F(\varsigma,\xi)$, then the Jacobian matrices of F^{-1} and F should satisfy the following equation,

$$\begin{bmatrix} \frac{\partial \varsigma}{\partial q} \\ \frac{\partial \xi}{\partial q} \end{bmatrix} \begin{bmatrix} \frac{\partial F}{\partial \varsigma} & \frac{\partial F}{\partial \xi} \end{bmatrix} = I_n\,. \tag{39}$$

In the next lemma we will determine the relationships between the derivatives of (ς,ξ) and that of the joint position q.

As the distribution $\Delta=ker\,(J)$ is involutive, the diffeomorphism F has the property, (see [13], p.27) that for every $q\in Q$, the r columns of the Jacobian matrix $\frac{\partial F}{\partial \varsigma}$ are linearly independent vectors in the distribution A. *O*

Lemma (The time derivatives of the transformed coordinates).

The transformation F given in lemma 5 allows us to write,

$$\dot{\xi}=M_J\, J\, \dot{q} \tag{40}$$

$$\dot{\varsigma}=M_N^{-1}\, N_J^T\, \dot{q}\,. \tag{41}$$

Proof : We can always find a nonsingular $r\times r$ matrix M_N, which expresses $\frac{\partial F}{\partial \varsigma}$ as a linear combination of the columns of N_J, thus,

$$\frac{\partial F}{\partial \varsigma} = N_J\, M_N\,. \tag{42}$$

From (39) we have $\frac{\partial \xi}{\partial q}\,\frac{\partial F}{\partial \varsigma}= 0$, thus, $\frac{\partial \xi}{\partial q}\, N_J\, M_N = 0\in IR^{m\times r}$. Hence N_J annihilates $\frac{\partial \xi}{\partial q}$. Recall that $JN_J=0$, thus each row of $\frac{\partial \xi}{\partial q}$ must be a linear combination of the rows of J. Hence,

$$\frac{\partial \xi}{\partial q}=M_J\, J\,. \tag{43}$$

Here M_J is a nonsingular $m\times m$ matrix. Therefore, $\dot{\xi}=\frac{\partial \xi}{\partial q}\dot{q} =M_J\, J\, \dot{q}$ yields equation (40). From (39) we have, $\frac{\partial \xi}{\partial q}\,\frac{\partial F}{\partial \xi}=I_m$. Combining this equation with (43) yields,

$$\frac{\partial F}{\partial \xi}=J^{+}M_J^{-1} \ , \tag{44}$$

because the nonsingular matrix J has a unique pseudo-inverse J^{+} such that $JJ^{+}=I_m$.

We can write, $\dot{q}=\frac{\partial F}{\partial \varsigma}\dot{\varsigma}+\frac{\partial F}{\partial \xi}\dot{\xi}$. Thus we have,

$$\frac{\partial F}{\partial \varsigma}\dot{\varsigma}=(I_n-\frac{\partial F}{\partial \xi}M_J\ J\ )\dot{q}=(I_n-J^{+}\ J)\dot{q}=P_J\ \dot{q}\ .$$

To obtain **(41)**, we substitute (42) into the above equation and premultiply both sides by N_J^T. Recall that $N_J^T N_J=I_r$, as each column of N_J is a normalized basis vector. ■

<u>Remark 3</u> : Equation (40) implies that $\dot{\xi}=M_J\dot{x}$ and $\frac{\partial \xi}{\partial x}=M_J$. From the implicit mapping theorem, the nonsingularity of M_J ensures that ξ is homeomorphic to x.

<u>Lemma 7</u> (The decomposition of the unperturbed system).

Using the transformation F given by lemma 5, we can write the unperturbed system $\dot{q}=v$ (v is expressed by (28)) as a cascade system in the following form,

$$\dot{\varsigma}=\lambda M_N^{-1}(N_J^T\ \nabla H)\ (q(\varsigma,e)) \tag{45}$$

$$\dot{e}+\gamma e=0 \tag{46}$$

The notation used in (45) means that N_J^T and ∇H are functions of (ς,e) through dependency on the joint variable q. O

Proof : The unperturbed system, equation **(28)**, is given by,

$$\dot{q}=J^{+}(\dot{x}_d-\gamma e)+\lambda P_J\nabla H \tag{47}$$

Equation (46) is obtained by premultiplying both sides of (47) by J and recalling $JP_J=0$. Similarly, equation (45) is obtained by premultiplying both sides of (47) by $M_N^{-1}N_J^T$ and recalling that $N_J^T J^{+}=0$. Recall that q can be decomposed into (ς,ξ) by F^{-1} given by (38) and ξ is homeomorphic to x. Thus ξ is homeomorphic to e because there is one to one mapping between x and e. Then e is independent of ς, so q can be decomposed into (ς,e). ■

<u>5.2 Stability of the Zero Dynamics</u>

<u>Lemma 8</u> (The stability of a cascade system).

Consider the unperturbed system (45) and (46) in hierarchical form, $\dot{\varsigma}=f(\varsigma,\xi)$ and, $\dot{\xi}=g(\xi)$. If the functions f and g are continuously differentiable, then $(\varsigma,\xi)=(0,0)$ is a locally asymptotically stable equilibrium of the system, if and only if $\xi=0$ is a locally asymptotically stable equilibrium of $g(\xi)$ and $\varsigma=0$ is a locally asymptotically stable equilibrium of $f(\varsigma,0)$. O

The proof of this lemma can be found in Vidyasagar **[27]**. ■

The equilibrium point of the cascade system given in lemma 7 is $e=0$, $\varsigma=\varsigma^*$. Where ς^* is the coordinates such that $(N_J^T\nabla H)(q(\varsigma^*,0))=0$. The equilibrium joint position q^* is then given by $q^*=F(\varsigma^*,0)$.

__Remark 4__ : Setting $e=0$ in (45) gives us the zero dynamics [6, 13], (assuming that the output of the system is e),

$$\dot{\varsigma}=\lambda M_N^{-1}(N_J^T \nabla H)\,(q(\varsigma,0)) \tag{48}$$

of the unperturbed system. The zero dynamics is defined on the manifold IR^r. Equations (41) and (48) lead to,

$$N_J^T \dot{q}=\lambda(N_J^T \nabla H)(q(\varsigma,0)) \qquad or, \quad P_J \dot{q}=\lambda(P_J \nabla H)(q(\varsigma,0))\,. \tag{49}$$

Notice that $q(\varsigma,0) \in Q_N$, also notice that $P_J\dot{q}$ represents the motion of $q \in Q_N$ without any change in x. Furthermore, equation (49) is defined on the manifold of $\{q=F(\varsigma,\xi) \mid \varsigma \in IR^r,\ e=0\}$. This zero dynamics manifold is also expressed by

$$Q_N=\{q \in Q \mid x_d=K(q) \text{ and } J\dot{q}=0\}\,, \tag{50}$$

and is indeed the self-motion manifold over $x_d=K(q_0)$. We observe that the identity $\dot{q}=(J^+J + P_J)\dot{q}$ is satisfied for any $q \in Q$. However on the self-motion manifold $\dot{x}=J(q)\dot{q}=0$, thus $\dot{q}=P_J\dot{q}$. Equation (49) can be rewritten as,

$$\dot{q}=\lambda(P_J \nabla H)(q) \qquad for\ all\ q \in Q_N\,. \tag{51}$$

Equation (51) will in fact express the "equivalent zero dynamics" in the joint space and it is defined on the manifold Q_N.

__Proposition 4__ (The boundedness of the unperturbed system).

The equilibrium point q^* of the unperturbed system is asymptotically stable if the equilibrium point $(\varsigma^*,0)$ of the zero-dynamics (51) is asymptotically stable.. The trajectory $q(t)$ of the unperturbed system starting from any finite initial configuration q_0 is bounded if the solution trajectory of the zero dynamics defined on the self-motion manifold $Q_N^{x_0}$ $=\{q \in C(q_0) \mid K(q)=K(q_0)=x_0\}$ is bounded. O

Proof : Lemma 7 asserts that the unperturbed system given by (47) can be decomposed into a cascade system. Then the asymptotic stability results are obtained immediately from lemma 8. ■

__Proposition 5__ (Boundedness of $q \in Q_N$ is guaranteed for a choice of H).

Let the objective function $H(q)$ be a quadratic of the form :

$$H(q)=\frac{1}{2}(q-q_C)^T M(q-q_C) \tag{52}$$

where q_C is fixed, and M is a symmetric positive definite matrix. Further let q_C be given in a set of isolated points. Consider the zero-dynamics,

$$\dot{q}=\lambda P_J \nabla H(q)=\lambda P_J M(q-q_C) \quad with \quad q \in Q_N\,. \tag{53}$$

The vector $q \in Q_N$ is bounded and $q \to q^*$ as $t \to \infty$ for every fixed q_C. Where q* is the optimal solution of the problem given by (6). O

Proof : Let the Lyapunov function candidate V be, $V=\frac{1}{2}(q-q_C)^T M(q-q_C)\ (q \in Q_N)$. The derivative of V with respect to time is, $\dot{V}=\lambda(q-q_C)^T M\, P_J M(q-q_C)$

$=\lambda||P_J M(q-q_C)||^2 \leq 0$, for $\lambda<0$, because the matrix P_J is a projector. Hence $q-q_C \in L^\infty$, in addition, because of the boundedness of q_C we have $q \in L^\infty$. Notice that the set $E=\{q \in Q_N \mid \dot{V}=0\}$ is the the set of equilibrium points of (53), and is therefore an invariant set. From **LaSalle's** extension of Lyapunov direct method [14], $q(t) \rightarrow q^*$ as $t \rightarrow \infty$ because q is in a bounded set. 8

Therefore if we choose the objective function H to be of quadratic form, then the trajectory of the unperturbed system is always bounded. If q_C is not on the self-motion manifold, then q^* may not be equal to q_C. The solution vector q' must be in the feasible region of the constraints of the optimization problem, in this case the feasible region is $Q_N^{q_0}$.

__Remark 5__ : The quadratic performance function defined in (52) ensures that the function v in (11)is locally Lipschitz. Θ

$$v(q)=\begin{bmatrix} J \\ N_J \end{bmatrix}^{-1} \begin{bmatrix} (\dot{x}_d-\gamma e) \\ \lambda N_J \nabla H \end{bmatrix} = [J^+ \mid N_J] \begin{bmatrix} (\dot{x}_d-\gamma e) \\ \lambda N_J M(q-q_C) \end{bmatrix} = J^+(\dot{x}_d-\gamma e)+\lambda P_J M(q-q_C) \tag{54}$$

Matrices J^+ and P_J are differentiable because of assumption (A2) and the fact that Mis a constant matrix. Recall that a continuously differentiable function is locally Lipschitz, hence the function given in (54) is differentiable with respect to q, and is **therefore** locally Lipschitz. ■

6. Example

__6.1 Manipulator Model__

In this section we will apply the proposed adaptive control law to a three degree of freedom RPR robot with one prismatic joint followed by two **revolute** joints (see Fig. 2). The structural parameters of the robot are given in the below table.

Variable	*Value*	*Definition*
m_1	0.5 Kg	Mass of first link
m_2	0.3 Kg	Mass of second link
m_L	5.0 Kg	Mass of carried load
l_1	1.0 m	Maximum length of the radial link
r_2	0.6 m	Length of second link

Table 1. Redundant Robot Link Parameters

The structure of the dynamical equation of the RPR robot is as given in (12). The manipulator consists of a **revolute** joint with angle ϕ_1 followed by a prismatic link of length r_1 and another **revolute** joint angle ϕ_2. We will denote by $S_1=\sin\phi_1$, $S_2=\sin\phi_2$, $S_{12}=\sin(\phi_1+\phi_2)$, and $C_1=\cos\phi_1$, $C_2=\cos\phi_2$, and $C_{12}=\cos(\phi_1+\phi_2)$. For **convenience** the joint vector will be denoted as $q=(r_1, \phi_1, \phi_2)$. We will also define the parameter vector θ which is related to the manipulator structural parameters as follows, $\theta_1=m_1+m_2+m_L$,

$\theta_2=(\frac{m_2}{2}+m_L)r_2$, $\theta_3=(\frac{m_2}{3}+m_L)\, r_2^2$, $\theta_4=m_1 l_1$, and $\theta_5=\frac{1}{3}m_1 l_1^2$. Then the inertia matrix $D(q;\theta)$ and the Coriolis matrix $C(q,\dot{q};\theta)$ are given as [7],

$$D(q;\theta) = \begin{bmatrix} \theta_1 & -\theta_2 S_{12} & -\theta_2 S_{12} \\ -\theta_2 S_{12} & \theta_1 r_1^2-\theta_4 r_1+2\theta_2 r_1 C_{12}+\theta_3+\theta_5 & \theta_2 r_1 C_{12}+\theta_3 \\ -\theta_2 S_{12} & \theta_2 r_1 C_{12}+\theta_3 & \theta_3 \end{bmatrix}$$

$$C(q,\dot{q};\theta) = \begin{bmatrix} 0 & -\theta_1 r_1\dot{\phi}_1-\theta_2(\dot{\phi}_1+\dot{\phi}_2)C_{12}+\frac{1}{2}\theta_4\dot{\phi}_1 & -\theta_2(\dot{\phi}_1+\dot{\phi}_2)C_{12} \\ 2\theta_1 r_1\phi_1 & 2\theta_2\dot{r}_1 C_{12}-\theta_4\dot{r}_1 & -\theta_2 r_1(2\dot{\phi}_1+\dot{\phi}_2)S_{12} \\ 2\theta_2\dot{\phi}_1 C_{12} & \theta_2 r_1\dot{\phi}_1 S_{12} & 0 \end{bmatrix}$$

Given that the reference velocity vector $v=(v_1,v_2,v_3)$, and the reference acceleration vector $a=(a_1,a_2,a_3)$, then the regressor matrix $Y(.)\in IR^{3\times 5}$ for this robot is given as,

$$Y(q,\dot{q};v,a)=\begin{bmatrix} -r_1\dot{\phi}_1 v_2+r_1 a_1 & y_{12} & 0 & \frac{1}{2}\dot{\phi}_1 v_2 & 0 \\ r_1^2+2r_1\phi_1 v_1 & y_{22} & a_2+a_3 & -\dot{r}_1 v_2-r_1 a_2 & a_2 \\ 0 & y_{32} & a_2+a_3 & 0 & 0 \end{bmatrix}. \tag{55}$$

where, we have set $y_{12} = -(a_2+a_3)S_{12}-(\dot{\phi}_1+\dot{\phi}_2)(v_2+v_3)C_{12}$, $y_{22} = 2\dot{r}_1 v_2 C_{12} -r_1(2\dot{\phi}_1+\dot{\phi}_2)v_3 S_{12} -a_1 S_{12}+2r_1 a_2 C_{12}+r_1 a_3 C_{12}$, and $y_{32} = 2\dot{\phi}_1 v_1 C_{12} +r_1\dot{\phi}_1 v_2 S_{12} -a_1 S_{12}+r_1 a_2 C_{12}$.

The robot end-effector positions x_1 and x_2 in the Cartesian space are given as, $x_1=r_1 C_1+r_2 C_{12}$ and $x_2=r_1 S_1+r_2 S_{12}$. The Jacobian is then expressed as $J = \begin{bmatrix} C_1 & -r\ S_1-r_2 S_{12} & -r_2 S_{12} \\ S_1 & r_1 C_1+r_2 C_{12} & r_2 C_{12} \end{bmatrix}$. Further the singular configurations are characterized by, $\det[JJ^T]=r_1^2(r_2^2 S_2^2+1)\ +2r_2 C_2(r_2 C_2+r_1)=0$. Thus the singularity occurs when $r_1=0$ and $\phi_2=(\pm 2k+1)\pi/2$, where k is any integer. In order to avoid singularity, we selected the objective function to keep link r_1 away from 0. The objective function was selected as, $H(q)=\frac{1}{2}[100(r_1-0.6)^2 +\phi_1^2 +\phi_2^2]$.

The basis vector of the null space of J is,

$$N_J=J_1^T\times J_2^T=[r_1 r_2 S_2,\ -r_2 C_2,\ r_1+r_2 C_2]^T\ . \tag{56}$$

The self-motion manifold for this manipulator can be computed for the specified $x_0=K(q_0)=K(q)$ by solving the differential equation given by (35). In this example the self-motion manifold will be represented by a curve in the three dimensional joint space for specified x_0.

6.2 The Example End-effector Trajectory

The end-effector of the manipulator was used to trace a circle of radius 0.2 m passing through (0.83, 0.19) with initial joint configuration $q(0)=(0.3, 0.7, -0.7)$. The circle was traced in a period of 5 seconds. For the adaptive control simulations, the initial estimates of the parameters were set at $\hat{\theta}(0)=(0, 0, 0, 0, 0)$. The actual values of the parameters of the manipulator are $\theta_{act}=(5.8, 3.09, 1.84, 0.5, 0.17)$, and the load mass $m_L=5$.

6.3 Stability of the Zero Dynamics

We will show that $r_1 \approx 0.6$ is the asymptotic optimal point and the zero dynamics is indeed stable. In order to do that, we computed the curve for the zero dynamics manifold given by the equation (35). In this example we used $x_0=(0.83,\ 0.19)$ and $q(0)=(0.3,\ 0.7,\ -0.7)$. The coordinates of the self-motion manifold, which is a connected curve in the three dimensional q coordinates, is obtained from the integration of the components of N_J. The arc length of the self-motion manifold traversed at time t is $s=\int_{u=t_0}^{t} ||N_J||\,du$. Therefore the arc length s is homeomorphic to time t. Fig. 3 shows the coordinates of q versus s, here $q=(r_1,\phi_1,\phi_2)$. Recall from the discussion in eections 2 and 5 that Nj is the tangent map of the self-motion manifold and from (51) the zero dynamics is given by $\dot{q}=\lambda P_J \nabla H = N_J(\lambda N_J^T \nabla H)$, where $\lambda N_J^T \nabla H$ is a scalar. Therefore the magnitude of the zero dynamics vector field on the self-motion manifold is represented by the scalar $v_s=<N_J\ ,\ \lambda P_J \nabla H> = \lambda N_J^T \nabla H$. We constructed the phase portrait of the zero dynamics with the plot of v_s versus s, for the initial values of $x_0=(0.83,0.19)$ and $q(0)=(0.3,0.7,-0.7)$. The scalar $\lambda N_J^T \nabla H$ is depicted by a solid line in Fig. 3. The attractive configurations are those joint configurations $q=q_e(s_e)$, where $v_s(q_e)=0$ and $\frac{dv_s}{ds}<0$ in the neighborhood of $s=s_e$. From Fig. 3, we see that the points A, , A_2 , A_3 are attractive equilibrium points, and the points B_1 , B_2 are repelling equilibrium points. At points A, , A_2 and A_3 we do indeed find that $r_1 \approx 0.6$. If we start from the initial condition $q(0)=(0.3,0.7,-0.7)$, then the motion of the joints will approach and stay at the point A:, (as A_2 is the first attractive equilibrium point on the self-motion manifold). Thus, we have shown numerically that r_1 approaches 0.6, and from proposition 5 this is also the point at which the function $H(q)$ is optimized locally as the projected gradient of His zero at A_2. Notice that if we have two different H functions (with different weighting on the quadratic) the slopes (i.e., $\frac{dv_s}{ds}$) of the phase portraits will be different, and faster convergence to A_2 will result for the one with the larger slope.

The above numerical demonstration of the stability can be verified from the equilibrium points of the zero-dynamics, equation (51), or, $\dot{q}=\lambda(\ 100 r_1 r_2 S_2(r_1-0.6)$ $-r_2 C_2 \phi_1\ +(r_1+r_2 C_2)\phi_2\ )$ Nj $=0$. This equation was numerically solved because analytical solutions are not easily obtained.

6.4 Simulations with the Non Adaptive Version of our Control Law

In order to provide a basis for comparison and to demonstrate the need for adaptive control, we simulated the control law given by (18) with the adaptation mechanism switched off and $w_i=1$. In the simulation the values of the parameters $\hat{\theta}=(1,1,1,1,1)$ are used in the control law calculations. These parameter values were held constant throughout the simulation. Notice that these parameters were different from the actual values. The responses of the manipulator joints are shown in Fig. 4. The tracking error $e=(e_1,e_2)$ is shown in Fig. 5. We see that there is a steady state tracking error for the simulated trajectory. This steady state error would disappear if the actual parameters are used in the control law calculations.

6.5 A Comparison with Other Redundant Robot Adaptive Control Schemes

We will compare the performance of our adaptive control law with that of Niemeyer and Slotine's adaptive scheme [19]. In their redundant robot adaptive scheme the joint reference velocity, q_r, and the joint reference acceleration, $\ddot{q}_r$ are computed from the desired end-effector position, x_d, and the actual position, x. Given $\dot{x}_r=\dot{x}_d-\Lambda(x_d-x)$ (A is a positive definite matrix), then the end-effector reference acceleration is $\ddot{x}_r=\ddot{x}_d-\Lambda(\dot{x}_d-\dot{x})$. These signals are used to compute the joint reference acceleration (see [19], section 3.2) as, $\ddot{q}_r=J^+(\ddot{x}_r-\dot{J}\dot{q}_r)+ P_J(\dot{\Psi}+\dot{J}^T(J^+)^T(\dot{q}_r-\Psi))$ and the joint reference velocity as $\dot{q}_r=J^+\dot{x}_r+P_J$ 3. The function Ψ is the gradient of the objective function f (see [19], section 3.2) and is described as $\Psi=-\lambda_s\nabla f$, (where X, is a positive constant). Further the objective function f is given as $f=\frac{1}{2}q^Tq$. The sliding vector $s=\dot{q}-\dot{q}_r$ is used in the control law (see [19], equation 4) $\tau=Y(q,\dot{q},\dot{q}_r,\ddot{q}_r)\hat{a}-K_Ds$, the parameter estimates $\hat{a}\in IR^r$ are calculated from equation 6 in [19] as $\hat{a}=-PY^Ts$. Here the matrix $Y\in IR^{n\times r}$ is the regressor matrix as described in our paper, and $P\in IR^{r\times r}$ is a positive definite gain matrix. Niemeyer and Slotine implemented their control scheme on a four-link redundant robot. They showed that the adaptive scheme had superior performance over a PD control scheme (see [19], Fig. 5), when the initial parameter estimates were set to zero, $\hat{a}(0)=0$. 'We applied the scheme of Niemeyer and Slotine to the example described earlier in this section in order to compare it with our adaptive scheme. The following gains were used in their control scheme, $K_D=50I_5$, $P=5I_5$, and $\lambda_s=50$.

Case 1: The parameter estimates $\hat{a}(0)$, (or in this paper $\hat{\theta}(0)$) are set to zero. In this case, the end-effector tracking error shown in Fig. 6 remains bounded and does not converge. The parameters which are shown in Fig. 7 do not appear to converge to any value for the period of time shown or for a larger period of time. The torques which are shown in Fig. 8 are acceptable. Therefore for this set of gains the controller given in [19] appears to behave much like our non-adaptive scheme.

Case 2: The controller given in [19] is simulated with the parameter update gain significantly increased, such that $P=200I_5$. The tracking error appears to converge to zero but the rate of convergence is slow, see Fig. 9. The parameters appear to get closer to their actual values, see Fig. 10.

6.6 Simulations with Our Adaptive Control Law

The full adaptive control law (18) was applied to the redundant robot given earlier. The reference vectors v and a are given by (28) and (29) respectively. The weighting function w_t was selected as $w_t^{-1}=0.1\exp(-bt)+0.02(t+1)^{-c}$, (with $b=2$ and $c=1.1$). Notice that $w_t^{-1}\in L^1$. The exponential term in w_t is used to improve the transient tracking error, the bigger the constant b, the faster the transient response becomes. The constant c is used to slow down the rate of increase of w_t, the smaller the constant c, the slower the rate of increase of w_t becomes. In the simulation, we selected a bound on $\hat{\theta}$ such as $\bar{\theta}=7$ and $\sigma_0=20$. We noticed that, $||\hat{\theta}||$ never reaches its maximum value of 7. The controller works well without the σ term. As external disturbances result in parameter drift, the σ term was initially added to prevent this drift. The controller gain $K_r=50I_3$, the matrix $\Gamma^{-1}=5I_5$, the constant $\lambda=-1$, and the initial condition $\hat{\theta}(0)=(0, 0, 0, 0, 0)$ were used in the simulation for the described trajectory. The manipulator joint responses are shown in Fig. 11. The end-effector tracking errors are shown in Fig. 12. The parameter estimates $\hat{\theta}(t)$ are shown in Fig. 13a, Fig. 13b and Fig. 13c. The control torques are shown in Fig. 14. We can see that the end-effector tracking errors tend to zero as $t \rightarrow \infty$. The parameter estimates are also seen to remain bounded. The simulations also show that the joint position responses remained bounded. The joint variable r_1 was initially set at 0.3 m and we see that r_1 converges to 0.6 almost immediately. From the analysis of the zero dynamics in sections 5 and 6.3, we know that $r_1 \approx 0.6$ is a stable equilibrium point, this was verified through the simulation. The objective function $H(q)$ is optimized at point A_2. We can see that a control input is applied to the prismatic joint r_1 to maintain its position, and effectively the revolute joints are used to trace the end-effector trajectory. Notice that the system has selected this condition through the prescribed control law. Only the desired end-effector position and its derivatives are specified as the input to the system.

In comparison to the scheme of Niemeyer and Slotine which yielded bounded tracking error response for $\Gamma^{-1}=5I_5$, (our Γ is the same as their P^{-1}), our controller yields fast convergence of the end-effector tracking error e. Also the parameters and joints errors remained bounded for the same gain. Much larger gains are in fact needed for Niemeyer and Slotine's scheme to obtain parameters and error convergence. Computationally our controller appears to be more complex from an implementation stand point. However, we gave clear theoretical justification as to why our controller works well. We should also note that our non-adaptive scheme produced bounded tracking error for the specified trajectory when the parameters were unknown. The tracking errors was similar to that of Niemeyer and Slotine's adaptive scheme for low adaptation gain.

7. Conclusion

In this paper we developed an adaptive control law for rigid joint redundant robots. The control scheme achieved redundancy resolution at the joint velocity level. Given an end-effector trajectory, the control scheme determined the joint velocity which ensured the end-effector trajectory was tracked. It was shown through the use of a scalar weighting function that the velocity tracking was asymptotic and that the estimated parameters were bounded. The boundedness of the joint motion, was established through the analysis of a perturbed dynamical system. This dynamical system was transformed into a cascade system where one of the transformed system variables was shown to be homeomorphic to the end-effector error, while the other one was shown to be homeomorphic to the self-motion variable. The equations of motion on the self-motion manifold were first determined and then directly linked to the zero dynamics. The stability of the zero dynamics was then linked to the boundedness of the joint motions. To our knowledge past work on the adaptive control of redundant robots did not rigorously address the stability of the motion on the self-motion manifold or systematically develop an adaptive control strategy as was given in this paper. Simulations were also performed for a planar redundant robot to illustrate the effectiveness of the proposed adaptive controller. Comparisons with another existing adaptive scheme was also given.

Future research in this area should address the effects of joint flexibility, unmodeled actuator dynamics and strategies for multiple redundant robots control.

□

References

1. C. Abdallah, D. Dawson, P. Dorato, and M. Jamshidi, "Survey of Robust Control for Rigid Robots," *IEEE Control System Magazine, V.11, No.2, pp.24-30*, 1991.
2. S. Ahmad and Y. Nakamura, "Workshop Report on "Theory and Application of Redundant Robots"," *1989 International Conference on Robotics and Automation, Scottsdale, Arizona, 1989.*
3. J. Baillieul, J.M. Hollerbach, and R.W. Brockett, "Programming and Control of Kinematically Redundant Manipulators," *Proceedings of the 1984 IEEE Decision and Control Conference pp.768-774, 1984.*
4. D.S. Bayard and J.T. Wen, "New Class of Control Laws for Robotic Manipulators," *International Journal Control, V. 47, N. 5, pp.1387-1406, 1988.*
5. R. Colbaugh, K. Glass, and H. Seraji, "An Adaptive Kinematics Algorithm for Robot Manipulators," *Proceedings of the 1990 American Control Conference, (San Diego), pp.2281-2286,* 1990.
6. A. DeLuca, "Zero Dynamics in Robotics Systems," in *Nonlinear Synthesis, Progress in Systems and Control Series,* pp. 68-87, Birkhauser, Boston, 1991.
7. E. Freund, "Fast Nonlinear Control with Arbitrary Pole-Placement for Industrial Robots and Manipulators," *International Journal of Robotics Research, V.3, N.l, pp. 65-78, 1982.*
8. J.K. Hale and J.P. LaSalle, "Differential Equations and Dynamical Systems," *New York: Academic Press,* 1967.
9. M.W. Hirsch and S. Smale, "Differential Equations, Dynamical Systems, and Linear Algebra," *Academic Press, New York,* 1974.
10. P. Hsu, J. Hauser, and S. Sastry, "Dynamic Control of Redundant Manipulators," *Journal of Robotic Systems, V.6, N.2, pp133-148, 1989.*
11. A. Ilchmann and D. H. Owens, "Adaptive Stability with Exponential Decay," *Systems and Control Letters, V.14, pp.437-443,* 1990.

12. P.A. Ioannou and P.V. Kokotovic, "Instability Analysis and Improvement of Robustness of Adaptive Control," *Automatica, V.20, pp.583-594,* 1984.

13. A. Isidori, *Nonlinear Control Systems,* 2nd Ed. New York: Springer-Verlag, 1989.

14. J.P. LaSalle, "Some Extensions of Liapunov's Second Method," *IRE Transactions on Circuit Theory, V. , p.520-527,* 1960.

15. A. Liegeois, "Automatic Supervisory Control of Configuration and Behavior of Multibody Mechanisms ," *IEEE Transaction on Systems, Man and Cybernetics V.SMC-7, pp.868-871,* 1977.

16. R.H. Middleton and G.C. Goodwin, "Adaptive Computed Torque Control for rigid Link Manipulations," *Systems and Control Letters V.lO, pp.9-16* , 1988.

17. Y. Nakamura and H. Hanafusa, "Optimal Redundancy Control of Robot Manipulators," *International Journal of Robotics Research, V.6, N.l, pp32-42, 1987.*

18. D.N. Nenchev, "Redundancy Resolution through Local optimization: a Review," *Journal of Robotic Systems, V.6, N.6, pp769-798, 1989.*

19. G. Niemeyer and J-J E. Slotine, "Adaptive Cartesian Control of Redundant Manipulators," *Proceedings of the American Control Conference, (San Diego), pp.234-241, June 1990.*

20. R. Ortega and M.W. Spong, "Adaptive Motion Control of Rigid Robots : A Tutorial," *Automatica, V.25, N.6, pp.877-888,* 1989.

21. H.L. Royden, "Real Analysis," *MacMillan, New York,* 1963.

22. *N*. Sadegh and R. Horowitz, "An Exponentially Stable Adaptive Control Law for Robot Manipulators," *IEEE Transactions on Robotics and Automation, V.6, N.4, pp.491-496,* 1990.

23. H. Seraji, "Configuration Control of Redundant Manipulators: Theory and Implementation," *IEEE Transactions on Robotics and Automation, V.5, N.4, pp.4 72-490,* 1989.

24. B. Siciliano, "Kinematic Control of Redundant Robot Manipulators: A Tutorial," *Journal of Intelligent and Robotic Systems, V.3, pp.201-212, 1990.*

25. Y.D. Song, R.H. Middleton, and J.N. Anderson, "Study on the Exponential Path Tracking Control of Robot Manipulators via Direct Adaptive Methods," *1991 IEEE International Conference on Robotics and Automation, pp.22-27,* 1991.

26. M.W. Spong and M. Vidyasagar, *Robot Dynamics and Control,* John Wiley & Sons, New York, NY , 1989.

27. M. Vidyasagar, "Decomposition Techniques for Large-Scale Systems with Nonadditive Interactions: Stability and Stabilizability," *IEEE Transactions on Automatic Control, V.AC-25, pp.779-779, 1980.*

28. D.E. Whitney, "Resolved Motion Rate Control of Manipulators and Human Prostheses," *IEEE Transactions on Man-Machine Systems V.MMS-10, pp.47-59, 1969.*

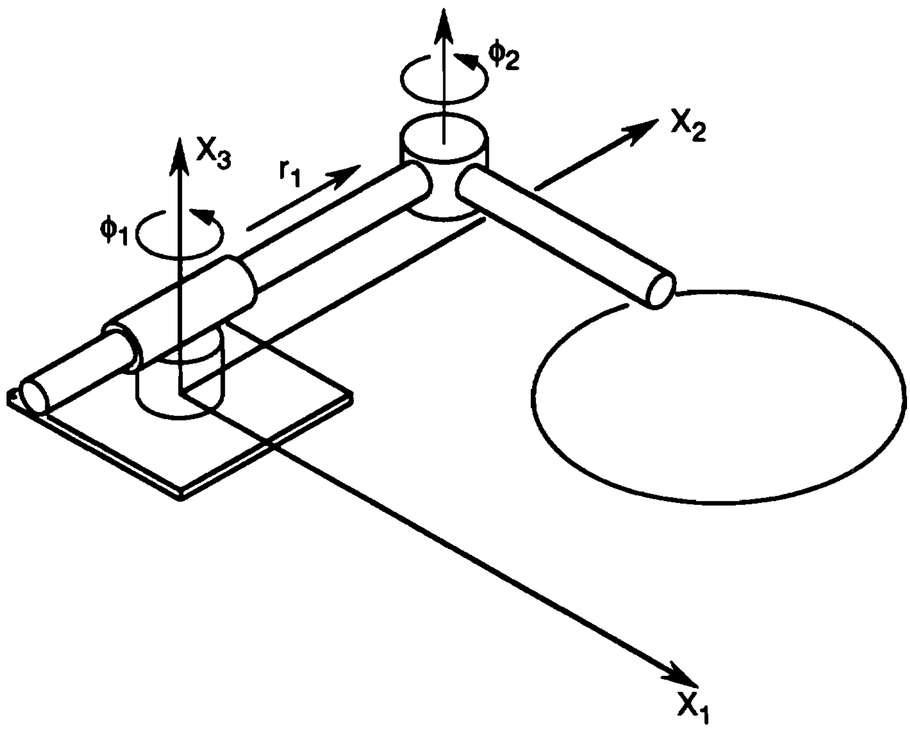

Fig 2. RPR Redundant Robot Tracing a Circle on the XY Plane

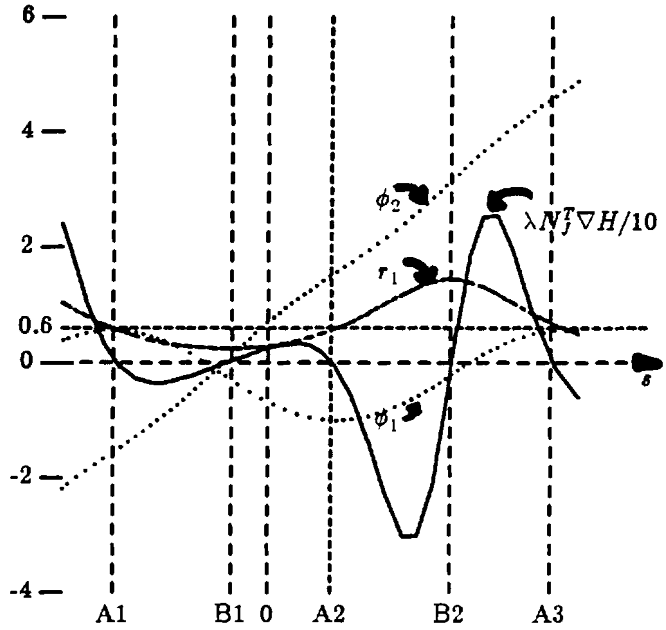

position

Fig. 3 Phase Portrait of the Zero Dynamics and the Joint Positions on the Self-Motion Manifold

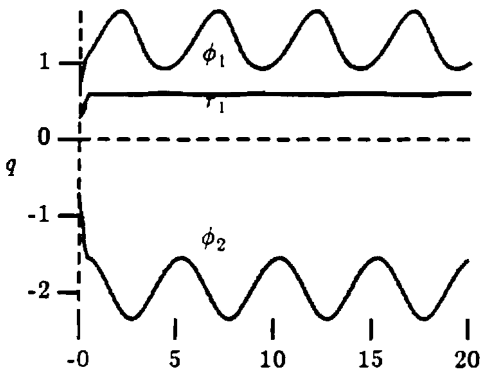

Fig. 4 Motion of the States for the Non-Adaptive case

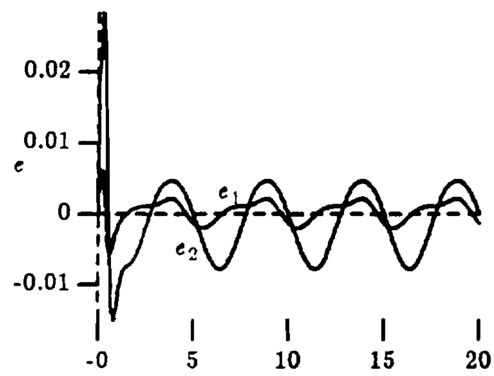

Fig. 5 Tracking Error for the Non-Adaptive case

May *30*, 1992

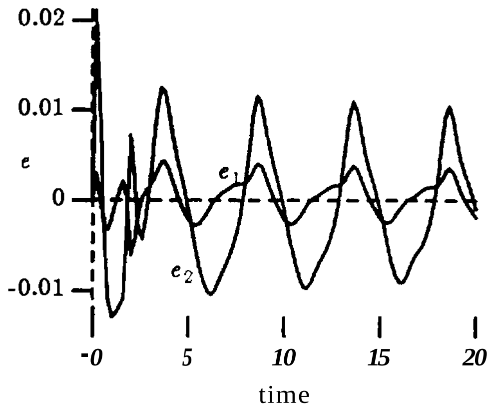

Fig. 6 Tracking Errors
For the scheme in [18] with $P=5I_5$

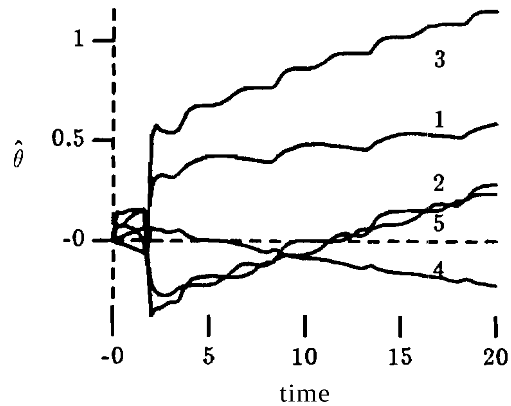

Fig. 7 Parameter Estimates
For the scheme in [18] with $P=5I_5$

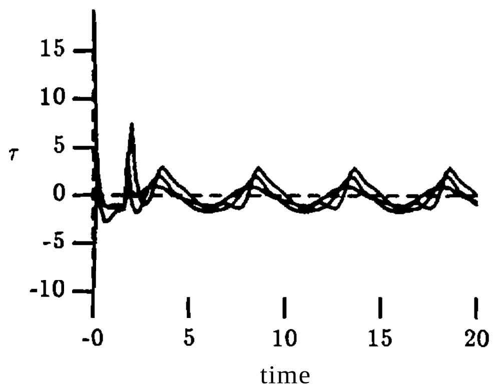

Fig. 8 Torques τ_1, τ_2, τ_3
For the scheme in [18] with $P=5I_5$

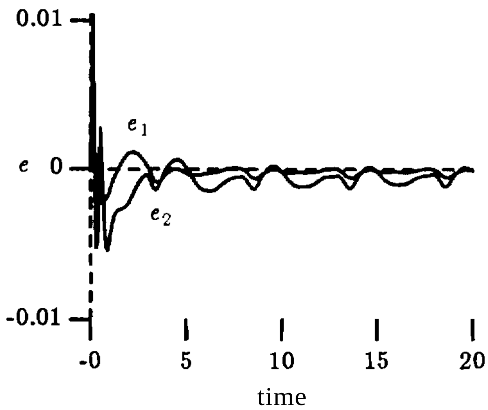

Fig. 9 Tracking Errors
For the scheme in [18] with $P=200I_5$

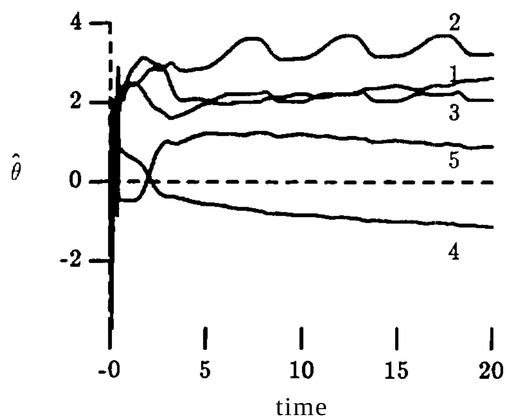

Fig. 10 Parameter Estimates
For the scheme in [18] with $P=200I_5$

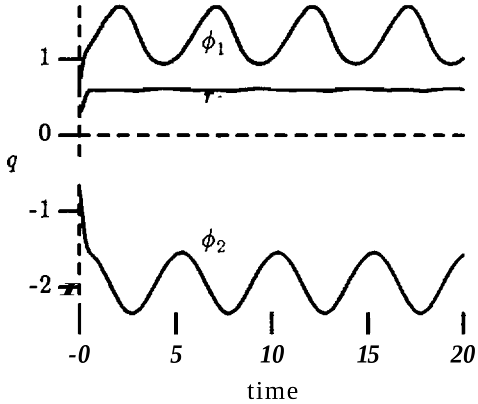

Fig. 11 Joint Motion
with $w_t^{-1} = 0.1e^{-2t} + 0.02(t+1)^{-1.1}$ *and* $\Gamma^{-1} = 5$

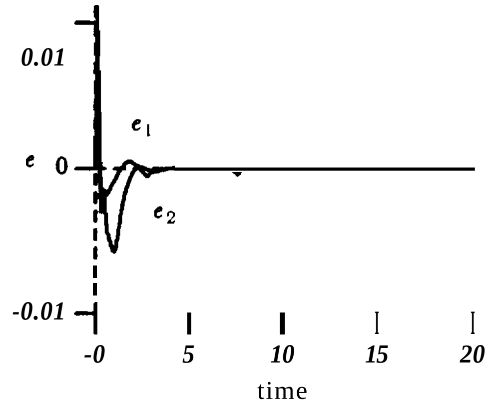

Fig. *12* Tracking Errors
with $w_t^{-1} = 0.1e^{-2t} + 0.02(t+1)^{-1.1}$ *and* $\Gamma^{-1} = 5$

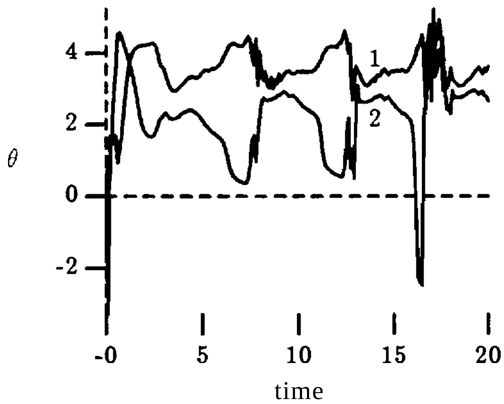

Fig. *13a* Parameter Estimates
with $w_t^{-1} = 0.1e^{-2t} + 0.02(t+1)^{-1.1}$ *and* $\Gamma^{-1} = 5$

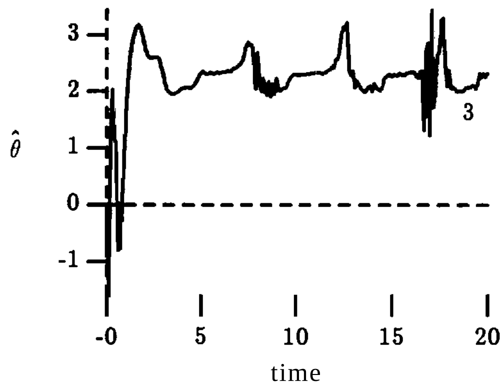

Fig. *13b* Parameter Estimates
with $w_t^{-1} = 0.1e^{-2t} + 0.02(t+1)^{-1.1}$ *and* $\Gamma^{-1} = 5$

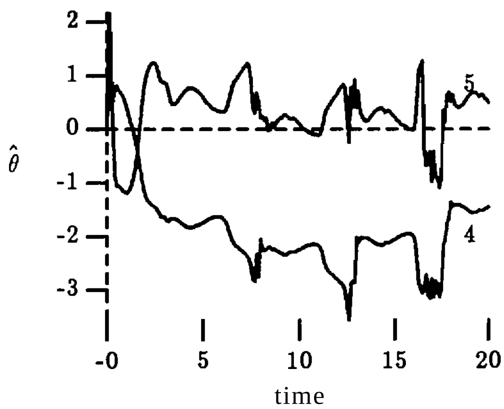

Fig. 13c Parameter Estimates
with $w_t^{-1} = 0.1e^{-2t} + 0.02(t+1)^{-1.1}$ *and* $\Gamma^{-1} = 5$

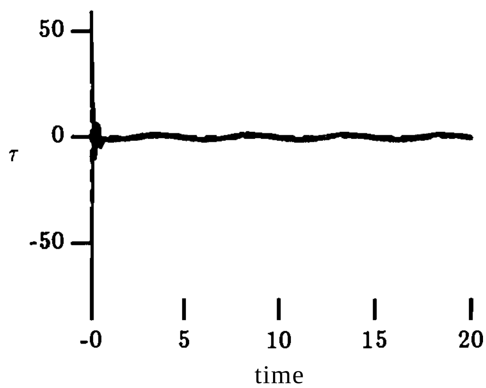

Fig. *14* Torques τ_1, τ_2, τ_3
with $w_t^{-1} = 0.1e^{-2t} + 0.02(t+1)^{-1.1}$ *and* $\Gamma^{-1} = 5$